〈論 文〉

A fine grid two-dimensional M_2 tidal model of the East China Sea

東支那海의 細格子 2次元 M_2潮汐模型

崔 秉 昊*
Choi, Byung Ho

Abstract

The previous two-dimensional non-linear tidal model of the East China Sea(Choi, 1980) has been further refined to resolve the flow over the continental shelf in more detail. The mesh resolution of the present finite-difference grid system used is 4 minutes latitude by 5 minutes longitude over the entire shelf. The developed fine grid two-dimensional model was utilized to reproduce the M_2 tide and M_4 tide for the East China Sea continental shelf. There is general agreement between the model results and the current observation made in the Eastern Yellow Sea, which supports the calculated tidal regime over the shelf. Some preliminary results on maximum bottom stress and tidally-induced residual current were also examined and discussed.

要 旨

陸棚上의 流動現象을 詳細하게 解像시키기 위해 旣 報告된 東支那海의 2次元 非線形潮汐模型(崔, 1980)을 緯度上 4分, 經度上 5分의 格子間隔을 갖는 有限差分格子體系로 改善시켰다. 樹立된 細格子模型은 東支那海의 M_2潮汐 및 M_4潮汐을 再現시키는데 一次的으로 利用되었는데 算定된 潮汐體系의 信賴性은 模型算定値와 黃海東側의 潮流觀測結果와의 全般的인 一致로서 立證되었다. 陸棚全體에 걸친 海底最大摩擦應力 및 潮汐恒流의 分布가 提示되었으며 또한 討議되었다.

INTRODUCTION

The East China Sea along with the Yellow Sea forms a complex oceanographic system with considerable spatial and temporal variations in physical properties and behaviour. There are major dynamic factors forcing this shelf sea: the tides, the surface wind and the Kuroshio, but the complexity of tidal phenomena is most remarkable in the region.

S. Ogura(1933), in his pioneering studies in this region, constructed cotidal and corange charts for diurnal and semidiurnal tides based on extensive coastal observations. The charts

* Department of Civil Engineering, Sung Kyun Kwan University, Suwon Campus, Suwon 170, Korea.

of Ogura have been proved to be remarkably accurate, despite the rather crude nature of available current observations. These charts together with coastal observations have been used as the basis of determining open boundary condition and overall verification of numerical modelling of tides in the region(An, 1977; Choi, 1980; Shen, 1980; Xia and Wang, 1984; Fang, 1985).

However there were no reliable long-term current measurement data to verify and to improve these tidal models. As the scientific interaction between China and the western world resume in the late 1970s, a cooperative field study of the Changjiang estuary and the East China Sea was initiated including the current meter moorings, once in 1980 and twice in 1981 (Larsen et al., 1985). Subsequently current measurement along a southern section of Shandong Peninsula was made by Woods Hole Oceanographic Institution during the course of investigating the wintertime circulation in November 1983. These current observations in the western Yellow Sea were then complemented by the recent current observations made in the eastern Yellow Sea during the winter of 1986 as a joint experiment by Florida State University and Sung Kyun Kwan University, Korea.

The need to understand tidal currents and storm surges in coastal areas with sufficient details and to predict changes in tidal regime that would be caused by large engineering developments accurately, has led to increased numerical modelling of tides in the East China Sea continental shelf.

In the present study the previous two-dimensional non-linear model of Choi (1980) has been refined to the resolution of 4 minutes latitude and 5 minutes longitude over the entire shelf to provide a general description of tidal motion and to identify many of the process that control these motions in more detailed manner.

HYDRODYNAMIC EQUATIONS

Considering the area covered by the model, the curvature of the earth and the variation with latitude of the Coriolis acceleration are taken into account by adopting spherical coordinates. The equations of motion and continuity as used in this model are(Flather, 1976; Choi, 1980):

$$\frac{1}{R\cos\phi}\left\{\frac{\partial}{\partial\chi}(Hu)+\frac{\partial}{\partial\phi}(Hv\cos\phi)\right\}+\frac{\partial\xi}{\partial t}=0, \quad \cdots\cdots(1)$$

$$\frac{\partial u}{\partial t}+\frac{u}{R\cos\phi}\frac{\partial u}{\partial\chi}+\frac{v}{R}\frac{\partial u}{\partial\phi}-\frac{uv\tan\phi}{R}-2\omega\sin\phi v+\frac{k_b u\sqrt{u^2+v^2}}{H}+\frac{g}{R\cos\phi}\frac{\partial\xi}{\partial\chi}=0, \quad \cdots\cdots(2)$$

$$\frac{\partial v}{\partial t}+\frac{u}{R\cos\phi}\frac{\partial v}{\partial\chi}+\frac{v}{R}\frac{\partial v}{\partial\phi}+\frac{u^2\tan\phi}{R}+2\omega\sin\phi u+\frac{k_b v\sqrt{u^2+v^2}}{H}+\frac{g}{R}\frac{\partial\xi}{\partial\phi}=0, \quad \cdots\cdots(3)$$

Equations (1)~(3) are vertically integrated hydrodynamical equations where the notations are.

t	time
χ, ϕ	east-longitue and latitude respectively
ξ	elevation of the sea surface above the undisturbed sea level
h	undisturbed depth of water
$H=h+\xi$	total depth of water
R	the radius of the Earth
ω	angular speed of the Earth's rotation
g	acceleration due to gravity
k_b	coefficient of bottom friction
u', v'	components of current in the directions of χ, ϕ respectively at a depth z below the undisturbed sea level

u, v components of depth-mean current given by

$$u=\frac{1}{h+\xi}\int_{-h}^{\xi}u'(z)dz,$$

$$v=\frac{1}{h+\xi}\int_{-h}^{\xi}v'(z)dz$$

These equations, formulated with a quadratic law of bottom friction, are integrated on a staggered finite difference grid using the scheme described by Roberts and Weiss(1967) which centers the advective terms in time and space. The method employed for implementing this scheme is described by Flather and Heaps (1975). Initial and boundary condition required for the solution of equations (1) to (3) are as follows:

At $t=0$: $u(\chi,\phi,t)$, $v(\chi,\phi,t)$ and $\xi(\chi,\phi,t)$ are specified for all positions at which the equations are to be solved.

At land boundary: the component of the flow normal to the boundary is permanently zero:

$$u\cos\theta+v\sin\theta=0$$

where θ is the angle between the normal to the coast directed out of the sea region and χ axis. Therefore

$u=0$ is the boundary condition at a ϕ-directed land boundary

$v=0$ is the boundary condition at a χ-directed land boundary.

Along an open boundary, elevation is specified as a function of time and position along the boundary: $\xi(\chi,\phi,t)$ is supplied.

As shown in Fig. 1 the grid spacing of the present fine grid model is about four nautical miles resulting from factor of three refinement of the grid system used in the previous coarse grid shelf model (Choi, 1980). The total number of grid point is over 35,000 and 60% of total grid are interior sea points. The time step for stable difference solutions according to the Courant-Friedrich-Lewy criterion was chosen as 69.003 seconds and has the period of the M_2 constituent as an integer number of

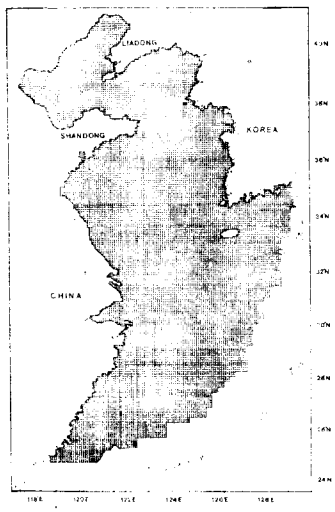

Fig. 1. Map of the East China Sea showing the 1/15° latitude and 1/12° longitude finite difference grid system.

time steps(648). The coefficient of bottom friction used has a value of 0.0025 uniformly over the region. The average depth for each grid was determined from navigational charts and depth contours corrected with referenced to mean sea level for model bathymetry is shown in Fig. 2. The basin receives large

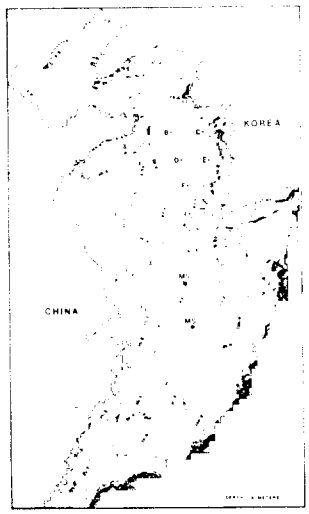

Fig. 2. The East China Sea continental shelf. The bathymetric contour interval is 10m showing the position of current meter rig of which mid-depth data are available.

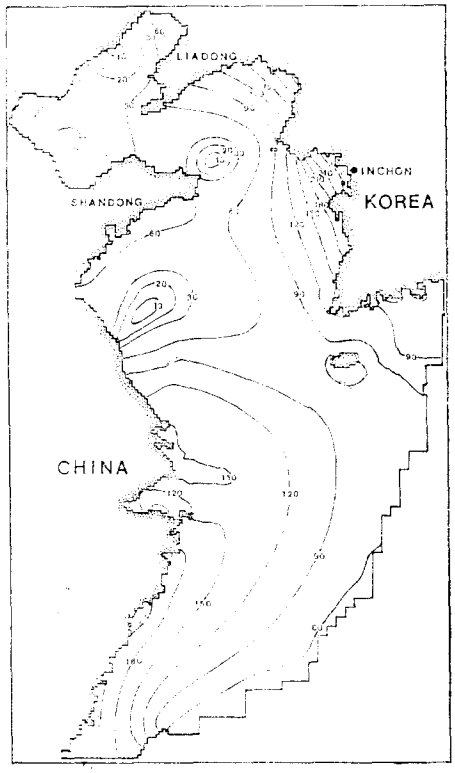

Fig. 3. Computed coamplitude chart for the M_2 tide (Values are given in cm).

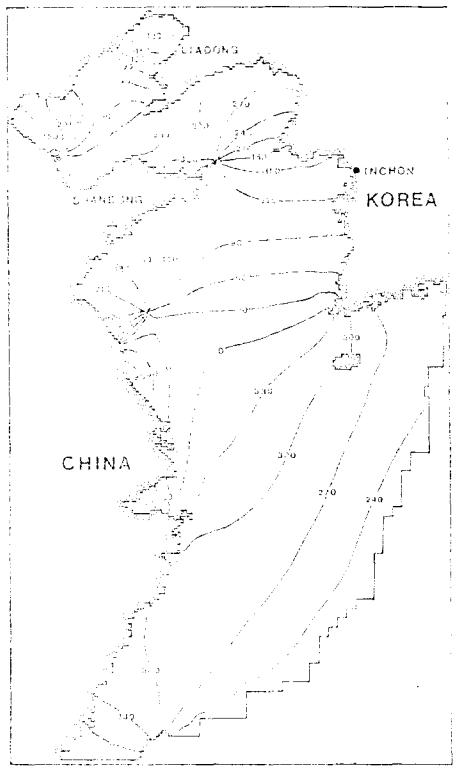

Fig. 4. Computed cophase chart for the M_2 tide (Values are given in degrees relative to the Moon's transit at 135°E)

amount of sediments from Huanho discharge and Changjiang river but relatively small amount of sediments from Korean rivers. The results is that the Yellow Sea basin is very shallow from the western to eastern side as illustrated in Fig. 2.

Along the open boundaries of the model, M_2 tidal input interpolated from the coarse grid two-dimensional model is specified. The cophase lines are given for time zone (GMT-9) hours following previous presentations(Ogura, 1933; Choi, 1980) for this region.

M_2 and M_4 TIDES

The results for M_2 tide obtained from the numerical model is shown in Fig. 3 and Fig. 4 as coamplitude and cophase charts respectively. Slightly improved amplitude values were obtained over the whole modelled region when comparing with previous coarse grid shelf model. These results will not be discussed further since they have been derived before(Choi, 1980). The numerical output for the M_4 tide is illustrated in Fig. 5 and Fig. 6. As seen in coamplitude chart, M_4 tidal amplitude is considerably high along the west coast of Korea and along the Chinese coast. In the west coast of Korea highest M_4 tides can be found in the Seohan Bay, the Inchon Bay and the estuary of Keum River. These show that the computed M_4 tide is the combination of contribution due to local nonlinear generation in the funnel-shaped estuaries and the presence of M_4 tide propagating along the west coast of Korea. The phase diagram corresponding to coamplitude lines is illustrated in Fig. 6 and

these cophase lines are proportional to the times of maximum elevation for the M_4 tide. The M_4 amphidromic spacing is about half the M_2 spacing and the tendency to develop nodal lines is well represented. Generally M_4 tide vary rapidly in the shallow areas where its generation is stronger. For this computation external propagation of M_4 tide through the modelled region is not considered since the M_4 tides at shelf edges are small. Computed current vectors also undergo harmonic oscillation and M_2, M_4 values of phase and current velocity are obtained by Fourier anlyzing each grid point for the M_2 and M_4 harmonics. In order to make coparison between computed and observed current, amplitudes and phases of easterly and northerly component of M_2, M_4 tidal currents were examined. In Table 1 and Table 2 computed and observed values of amplitude H(cm/sec) and phase κ(degree referred to 135°E) of the M_2 and M_4 tidal currents for six current meter data positioned at mid-depth are given. Tidal harmonic analysis of the east and north component of current was performed by the standard least square algorithm used at Bidston for routine analysis of coastal tidal elevation time-series(Choi, 1984). It is seen from these tables that generally good agreement between the observations and model results have been demonstrated.

These computed tidal currents can best be represented by the M_2 and M_4 tidal current ellipses as illustrated in Fig. 7 through Fig. 10. These ellipses give an overall impression of the magnitude and direction of the M_2 and M_4 tidal current distribution representing the

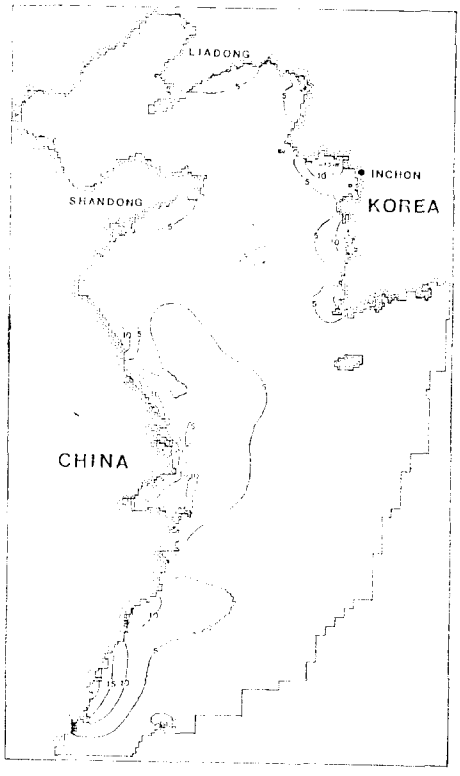

Fig. 5. Computed coamplitude chart for the M_4 tide (Values are given in cm).

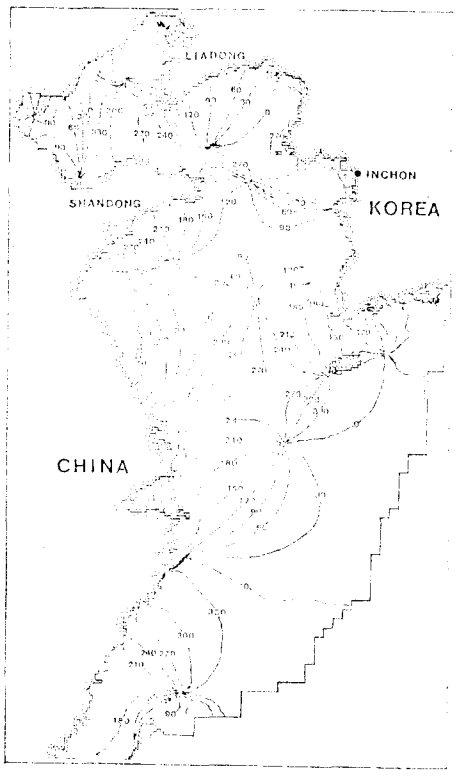

Fig. 6. Computed cophase chart for the M_4 tide (Values are given in degrees relative to the Moon's transit at 135°E).

Table 1. Comparison of observed and computed amplitudes (cm/sec) and phases (degree referred to 135°E) for u and v component of M_2 tidal current.

Current meter rig	Observed				Calculated			
	u		v		u		v	
	H	κ	H	κ	H	κ	H	κ
B	18.6	26	32.8	168	18.5	48	26.7	168
D	15.2	32	26.1	84	14.2	42	26.6	82
F	5.0	28	40.0	40	9.1	53	40.6	47
I	13.4	132	43.8	19	13.1	153	45.6	26
M5	47.3	107	50.8	11	58.0	93	53.9	2
MS	42.2	83	40.7	345	48.5	64	38.0	317

* B, D, F, I data were from the Eastern Yellow Sea mooring(Harkema and Hsueh, 1987).
** M5, MS data were from U.S.—China joint field study (Larsen et al., 1985)

Table 2. Comparison of observed and computed amplitudes (cm/sec) and phases (degree referred to 135°E) for u and v component of M_4 tidal current.

Current meter rig	Observed				Calculated			
	u		v		u		v	
	H	κ	H	κ	H	κ	H	κ
B	0.8	20	0.5	162	0.8	6	1.1	207
D	1.1	11	0.3	11	0.6	20	0.5	262
F	0.7	65	0.9	345	0.9	79	1.0	356
I	1.4	58	0.4	31	1.2	96	1.2	19
M5	1.4	213	0.6	173	1.7	332	1.6	215
MS	3.1	241	2.0	174	2.0	266	1.4	146

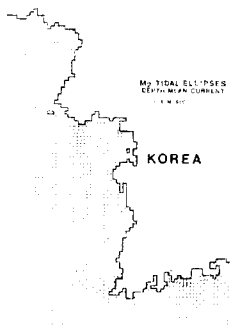

Fig. 7. Computed principal axes of the M_2 tidal current ellipses for the Eastern Yellow Sea.

maximum and minimum velocities as semi-major and semi-minor axis respectively. In near coastal areas of Sehan Bay, Inchon Bay, southwestern tip of Korean Peninsula and Hangzhou Bay, elongated M_2 major axes representing strong rectilinear currents already presented in the coarse grid shelf model are again well demonstrated with sufficient details. M_4 tidal current ellipses also clearly illustrate the considerable magnitude in the strong M_2 current region suggesting the interaction between the two component of tides. In shallow bays the maximum M_2 and M_4 tidal currents tend to be aligned in the same direction in medial axis of

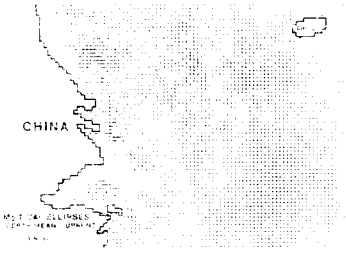

Fig. 8. Computed principal axes of the M_2 tidal current ellipses for off Changjiang River Estuary.

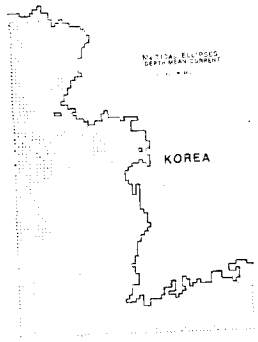

Fig. 9. Computed principal axes of the M_4 tidal current ellipses for the Eastern Yellow Sea.

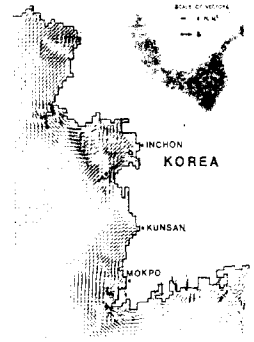

Fig. 11. Distribution of computed maximum bottom stress over the Eatern Yellow Sea.

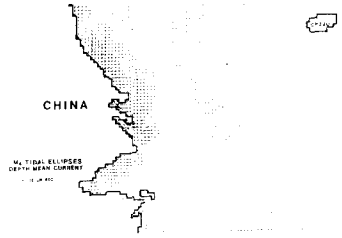

Fig. 10. Computed principal axes of the M_4 tidal current ellipses for off Changjiang River Estuary.

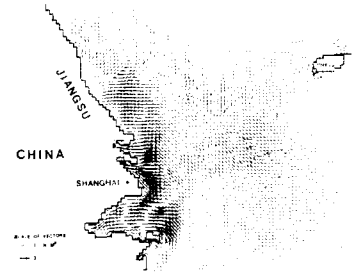

Fig. 12. Distribution of computed maximum bottom stress over off Chanjiang River Estuary.

channels.

The M_2 and M_4 tidal currents combine to give differences in peak flood and determined from the numerical models are remarkably similar to the sand transport paths in the North Sea and the East China sea continental shelf respectively based on geological evidence (Pingree and Griffiths, 1979; Choi, 1986).

The inferrence used in the previous studies was that the directions of computed maximum bottom stress and the net sand transport directions which would result from calculating the integral over the semi-diurnal tidal cycle, of the cube of current speed minus threshold, using the same computed current would be the same.

Using the present fine grid model the distri bution of maximum bottom stresses, following the numerical methods of Uncles(1983) which includes the effecs of residual flows as well as peak stress due to M_2 and M_4 interactions, in the Eastern Yellow sea and off Changjiang River estuary have been plotted as illustrated in Fig. 11 and Fig 12 respectively. The maximum bottom stress is computed as peak current speed squard, times a drag coefficient optimally adjusted as 0.0025.

Strong peak stress vectors can be seen in Seohan Bay, Inchon Bay, southwest corner of Korean peninsula, off Jiangsu coast and Hangzhou Bay where the distinguished offshore tidal sand banks occur. It is worth noting that noticeable divergence of stress vectors denoting bed-load parting can be seen in abovementioned strong current region.

The present results could be utilized to conform the earlier predictons of sand transport directions of the offshore tidal sand banks over the Yellow Sea based on diagrammatical method suggested by Kenyon et al. (1981) and peak stress vectors from the coarse grid shelf model. Modern accumulation of fine-grained material in the southern area of Cheju Island

discussed by Millimam et al. (1985) can be explained by both influx of sediment from the northwest during winter storms and continual resuspension transport by M_2 M_4 tides throughout the year. This previous inference can be further supported by present model results.

RESIDUAL CURRENTS

Residual currents are from meteorological (wind stress, atmospheric pressure gradient), thermohaline (density gradient) and hydrological (river flow) forcing, of tidal origin. The tide-induced residual currents can dominate dispersive mechanism in regions of modest fresh water input and moderate wind forcing.

Tidal eddies are generated by the transfer of vorticity from the tidal component of vorticity to the mean flow as a consequance of the advective or field accelerlation terms in the equation of motion and these effects are often associated with strong oscillatory flows around complex coastline configurations. Davies(1983) has shown that, unlike the meteorologically-induced residual flow, the horizontal pattern of tidal residual circulation form the three-dimensional model does not vary significantly through the vertical. For this reason tidal residual derived from the vertically integrated two-dimensional model will give general circulation pattern. However, in the literature one may find several definitions of residual currents and different method of computation (Nihoul and Ronday, 1975; Cheng and Casulli 1982; Zimmerman, 1979).

In the present study the tidal circulation is first computed in a conventional way. In Fig. 13 Eulerian residual currents over the shelf are obtained by integrating the depth-mean current over one lunar tidal period. Model-computed currents and observed residual from the Eastern Yellow Sea moorings are in general agreement in direction and magnitude(<3~4

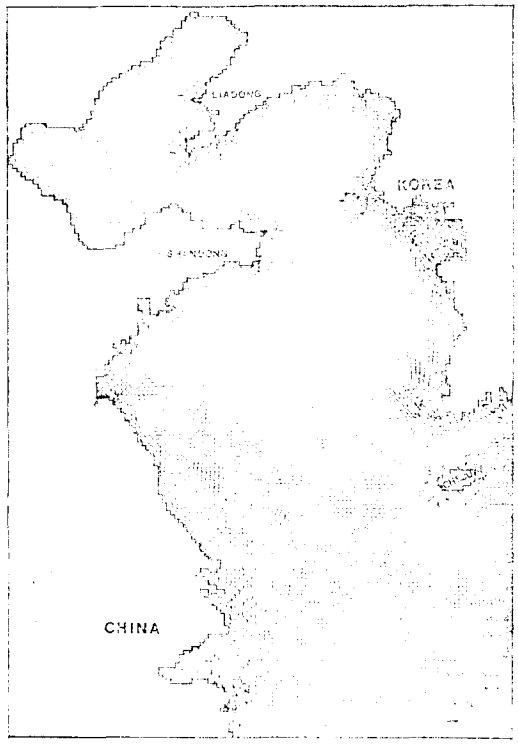

Fig. 13. Eulerian tidal residual currents computed from the model

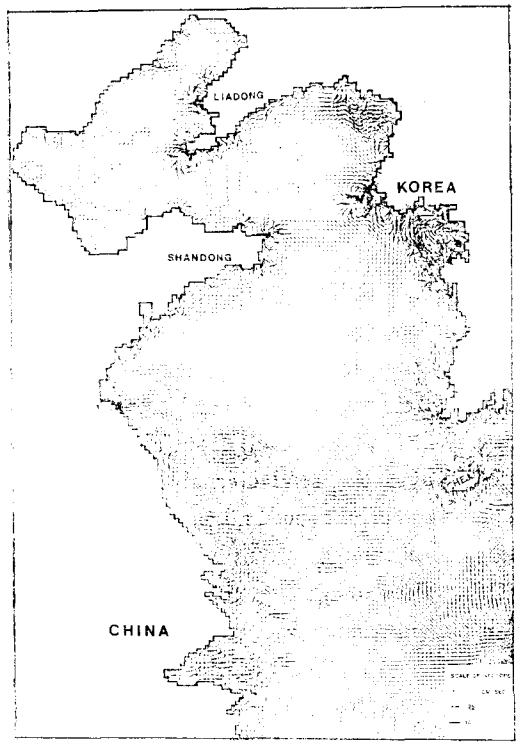

Fig. 14. Eulerian tidal residual transport velocity computed from the model.

cm/sec for off west coast of Korean Peninsula). It is seen from this figure that there are a number of strong eddies which appear to be generated in inner region of following 50m depth contour and upward strong tidal residuals are associated with the coastal areas of mid-Chinese coast. Generally, computed residuals are an order of the magnitude less than the tidal currents over the region. In Fig. 14 Eulerian residual transport velocity defined as first order Lagrangian residual current (Cheng, Feng and Xi, 1986), the sum of the Eulerian residual current and the Stokes drift is illustrated. As seen from both figures, tidal circulation is weak in the central part of the Yellow Sea and similar circulation pattern from both diagram except shallow water region due to the contribution from the Stokes drift. A very slow cyclonic gyre-like circulation in the middle part of the Yellow Sea may be due to the weak tidal residual current and sense of anticlockwise rotation of M_2 currents. It is worth nothing that basin-scale anticlockwise eddies are presented in Seohan Bay and Inchon Bay. At present tidal circulation in the shelf is largely unknown and subject to future extensive studies including satellite-tracking buoy studies and alternative ways of evaluations.

CONCLUDING REMARKS

Increasing computational facilities in recent years and the need to resolve the flow with sufficient details have enabled to develop a considerably fine grid tidal flow model in the Easa China Sea.

Preliminary results of a fine grid two-dimensional numerical model of the tidal motions in the East China Sea have been presentedt. It was demonstrated by this model that the computed M_2 and M_4 tidal currents were in good agreement with limited current observations made at mid-depth. Maximum bottom stress vectors due to M_2 and M_4 tides derived from the present model reconfirmed the previous results from the coarse grid shelf model with enhanced flow resolution.

Tidally-induced residual currents were also illustrated and compared with limited field observation. Extensive offshore tidal observations and current measurements together with modelling effort are essential for the better understanding of the tidal dynamics in this shelf sea.

ACKNOWLEDGEMENTS

The joint Eastern Yellow Sea current observation program was funded by the Korea Science and Engineering Foundation and numerical computations by IBM 3083 was supported by the Software Engineering Center at System Engineering Research Institute KAIST.

References

1) An, H.S. (1977), A numerical experiment of the M_2 tide in the Yellow Sea. Journal of Ocea nogarphical Society of Japan, 33(2), pp.103~110.

2) Cheng, R.T. and V. Casulli(1982), On Lagrangian resisdual currents with applications in South San Fransisco Bay, California. Water Resources Research, 18(6), pp.1652-1662.

3) Cheng, R.T., Feng, S. and P. Xi(1986), On Lagrangian residual ellipses. Lecture Notes on Coastal and Estuarine Studies, Vol.16, Physics of Shallow Estuaries and Bays (ed. J. van de Kreeke), Springer-Verlag.

4) Choi, B.H. (1980), A tidal model of the Yellow Sea and the Eastern China Sea. Korea Ocean Research and Development Institute Report 80-02, 72p.

5) Choi, B.H. (1984), Analysis of tidal observations at Major Ports around Korean Coast. Journal of Korean Society of Geodesy, Photogrammetry and Cartography, Vol.2, No.1, pp.17~33.

6) Choi, B.H. (1986), Predictions of sand transport

directions of the offshore tidal sand banks in the Yellow Sea. Proceedings of 5th APD/IAHR, Seoul, Korea, pp.231~247.

7) Davies, A.M.(1983), Applicationof a three-dimensional shelf model to the calculation of North Sea currents. in North Sea Dynamics(ed. Sündermann, J. and Lenz, W.), pp.44-62.

8) Fang, G.(1985), A finite-difference-least square technique for solving tidal wave equations with specific application to the modelling of M_2 tide in the Huanghai Sea. Scientia Sinica(B), 28 (10), pp.1110-1120.

9) Flather, R.A.(1976), A tidal model of the North-West European continental shelf. Memoires de la Societe Royale des Sciences de Liege, Ser. 6, 10, pp.141~164.

10) Harkema, R. and Y. Hsueh (1987), A complilation of moored current meter data in the Eastern Yellow Sea, January-April 1986. Department of Oceanography, Florida State University, Technical Report CMF-87-01.

11) Kenyon, N.H., Belderson, R.H., Stride, A.H. and M.A. Johnson(1981), Offshore tidal sand banks as indicators of net sand transport and as potential deposits. in Holocene marine sedimentation in the North Sea basin (ed. Nio, S.D., Schuttenheim, R.T.E., van Weering, T.C.E.), Int. Assoc. Sedimentelogist, Spec. Pub. 5, pp. 257~268.

12) Larsen, L.H., Cannon, G.A. and B.H.Choi (1985), East China Sea tide current. Continental Shelf Research, Vol.4, Nosl/2, pp.77-103.

13) Milliman, J.D., Beardsley, R.C., Yang, Z. S. and R. Limeburner(1985), Modern Hunghe-derived muds on the outer shelf of the East China Sea: Identification and potential transport mechanisms. Continental Shelf Research, Vol.4, Nos, 1/2, pp.175-188.

14) Nihoul, J.C.J. and F.C. Ronday(1975), The influence of tidal stress on the residual circulaiton, Tellus, 27, pp.484~489.

15) Ogura, S.(1933), The tides in the seas adjacent to Japan. Bulletin of the Hydrographic Department, Imperial Japanese Navy, V.7, 189p.

16) Pingree, R.D. and D.K. Griffiths(1979), Sand transport paths around the British Isles resulting from M_2 and M_4 tidal interactions. J. Mar. Biol. Ass. U.K., V.59, pp.497~513.

17) Roberts, K.V. and N.O. Weiss(1967), Convective difference schemes. Math. Comput., V.20, pp.272~299.

18) Shen, Y.(1980), Numerical computation of tides in the East China Sea. Journal of Shandong College of Ocenology, 11(1).

19) Uncles, R.J.(1983), Modeling tidal stress, circulation and mxing in the Bristol Channel as a prerequiste for ecosystem studies. Canadian Journal of Fisheries and Aquatic Sciences(Supplement), V.40, pp.8~19.

20) Xia, Z. and Z. Wang(1984), A numerical model of the M_2 constituents in the Huanghai Sea. Journal of Oceanography of Huanghai and Bohai Seas, 2(1).

21) Zimmerman, J.T.F.(1979), On the Euler-Lagrangian trasformation and the Stokes drift in the prerence of oscillatory and residual currents Deep Sea Research, 26A, pp.505~520.